



OPEN Co-substrate model development and validation on pure sugars and corncob hemicellulosic hydrolysate for xylitol production

Juan Feng^{1,2}, Charin Techapun^{1,2}, Yuthana Phimolsiripol^{1,2}, Pornchai Rachtanapun^{1,2}, Suphat Phongthai^{1,2}, Julaluk Khemacheewakul^{1,2}, Siraphat Taesuan^{1,2}, Kritsadaporn Porninta^{1,2}, Su Lwin Htike^{1,2}, Chatchadaporn Mahakuntha^{1,2}, Sumeth Sommanee^{1,2}, Rojarej Nunta^{1,4}, Anbarasu Kumar³ & Noppol Leksawasdi^{1,2}✉

A co-substrate model of *Candida tropicalis* TISTR 5306 cultivated in 10 - 100 g/L xylose and 1 - 10 g/L glucose at the ratio of 10:1 was developed based in part on modified Monod equation. The kinetic parameters include substrate limitation as well as substrate and product inhibitions with inclusion of threshold values. A general good fitting with average RSS_{total} , R^2 , and MS_{total} values of 162, 0.979, and 10.8, respectively, was achieved between ten simulated profiles and experimental kinetics data. The implementation of developed model on xylitol production from non-detoxified corncob hemicellulosic hydrolysate resulted in relatively good agreement with RSS_{total} , R^2 , and MS_{total} values of 368, 0.988, and 24.5, respectively. The developed model can be applied to predict microbial behavior in batch xylitol production system using hemicellulosic hydrolysate over a xylose range of 10 - 100 g/L and provide useful information for subsequent design of fed-batch and continuous systems to achieve the efficient sustainable resource management of this agricultural and agro-industrial waste.

Keywords Co-substrate cultivation, Model development, *Candida tropicalis*, Hemicellulosic hydrolysate, Xylitol production

Abbreviations

K_{ip}	Substrate inhibition constant associated with xylitol production (g/L)
K_{is}	Substrate inhibition constant associated with substrate utilization (g/L)
K_{ix}	Substrate inhibition constant associated with growth (g/L)
K_{sp}	Substrate limitation constant associated with xylitol production (g/L)
K_{ss}	Substrate limitation constant associated with substrate utilization (g/L)
K_{sx}	Substrate limitation constant associated with growth (g/L)
MS	Mean square
P	Xylitol concentration (g/L)
P_{ip}	Threshold xylitol concentration to inhibit xylitol production (g/L)
P_{is}	Threshold xylitol concentration to inhibit substrate utilization (g/L)
P_{ix}	Threshold xylitol concentration to inhibit growth (g/L)
P_{max}	Maximum xylitol concentration (g/L)
P_{mx}	Maximum xylitol concentration to inhibit growth (g/L)
P_{ms}	Maximum xylitol concentration to inhibit substrate utilization (g/L)
P_{mp}	Maximum xylitol concentration to inhibit xylitol production (g/L)
Q_p	Volumetric productivity of xylitol production (g/L/h)
Q_x	Volumetric productivity of biomass production (g/L/h)
$q_{s,max}$	Maximum specific substrate utilization rate (g/g/h)

¹Center of Excellence in Agro Bio-Circular-Green Industry (Agro BCG), Faculty of Agro-Industry, Chiang Mai University, Chiang Mai 50100, Thailand. ²Faculty of Agro-Industry, Chiang Mai University, Chiang Mai 50100, Thailand. ³Department of Biotechnology, Periyar Maniammai Institute of Science & Technology, Thanjavur 613403, India. ⁴Division of Food Innovation and Business, Faculty of Agricultural Technology, Lampang Rajabhat University, Lampang 52100, Thailand. ✉email: noppol@hotmail.com

$q_{p,max}$	Maximum specific xylitol production rate (g/g/h)
R^2	Correlation coefficient
RSS	Residual sum of squares
S_1	Xylose concentration (g/L)
S_2	Glucose concentration (g/L)
x	Biomass concentration (g/L)
$Y_{x/s}$	Xylitol yield based on sugar consumption (g/g)
$Y_{p/s}$	Biomass yield based on sugar consumption (g/g)
α	Proportioning factor for xylose consumption
μ_{max}	Maximum specific growth rate (h^{-1})

Xylitol is extensively utilized in the food and pharmaceutical industries due to its advantageous properties for human consumption¹. The economic value of xylitol is one of the highest among the well-accepted green chemicals. The xylitol market size was ever expanding with values at 906 million USD in 2021, 929 million USD in 2022, and 957 million USD in 2023 (Custom Market Insights). The CAGR of higher than 3.7% is expected to be achieved between 2024 and 2032. These are driven by the rising demand for natural and low-calorie sweeteners reflecting the health consciousness among consumers². Currently, research into microbial production of xylitol has been extensively explored as a viable alternative to chemical methods. Microbial production has advantages in terms of sustainability, environmental friendliness, efficiency, and production safety³.

Agro-industrial and agricultural wastes are the main contributors of lignocellulosic biomass, which have been extensively researched for its structural compositions and renewable properties⁴. Xylose-rich solution, which generally contains pentoses (xylose and arabinose) and hexoses (glucose, mannose, and galactose) is easily obtained by acid pretreatment and can be utilized as substrate for the production of xylitol^{4,5}. During the cultivation using sugar mixtures, a common observation is the inhibition or slowing down of D-xylose utilization, along with the suppression of xylose reductase (XR) synthesis due to the presence of glucose in the growth medium. In fact, many studies on mixture sugars cultivation have shown that the presence of excess glucose has detrimental effects on xylose metabolism and xylitol production. Whereas a low level of glucose could serve as a co-substrate to promote cells growth, supplies reduction equivalents, and maximizes the bioconversion of xylose into xylitol⁶. The higher xylitol production has been reported with an optimal xylose and glucose ratio of 10:1 by using *Pichia fermentans*^{6,7}, *Candida mogii*⁸, *C. magnoliae*⁹, and *Debaryomyces hansenii*¹⁰. Among microbial strains studied for their potential in xylitol production, *C. tropicalis* has been widely used due to its capability to metabolize pentoses, compatibility to almost all types of hemicellulosic hydrolysate, and high efficiency for bioconversion¹¹.

A modeling approach can provide insights into the factors influencing xylitol production kinetics, enhancing understanding of the process, and optimizing xylitol production strategies. For instance, the dynamic reaction kinetics of xylitol production using *C. tropicalis* ATCC 13,803¹² and *Kluyveromyces marxianus* ATCC 36,907¹³ were effectively characterized by the modified Monod equations. This model highlighted the impact of oxygen levels and xylose concentrations as limiting factors during the cultivation process. Yeast growth and xylitol production using *D. hansenii* ITB CCR85 cultivated in co-substrate of xylose and glucose were well modelled by Monod and Luedeking Piret kinetics, respectively¹⁴. Additionally, the kinetics of glucose and xylose mixture under the ratio of 3.5:1 cultivation using *C. tropicalis* MTCC 184 cultivated in sugarcane bagasse hydrolysate could also be reasonably described by Monod model. The comparative analysis of the model parameters provides a tangible understanding of how ultrasound irradiation influences xylitol production¹⁵. However, the kinetics and mathematical model of xylitol production using *C. tropicalis* with the optimal 10:1 xylose:glucose have not been fully characterized. This study is the first report for detailed mathematical development of xylitol production kinetics using *C. tropicalis* cultivated in 10:1 xylose and glucose mixture with incorporation of important kinetic parameters such as threshold and maximum xylitol concentrations inhibiting substrate consumption and xylitol production in the model.

In this study, ten batch conversions of *C. tropicalis* TISTR 5306 at various initial concentrations of pure xylose and glucose under the ratio of 10:1 was assessed. Xylitol production from non-detoxified corncob hemicellulosic hydrolysate in a batch culture system was assessed. The main objectives were to develop a co-substrate model of xylose and glucose at a ratio of 10:1, search for optimal kinetics parameters, and validate the developed model by interpolation and extrapolation to independent experimental kinetics data of pure sugars substrate. The assessment of model predictability was also extended by extrapolating validation to independent kinetic data using digested hemicellulosic hydrolysate as substrate for xylitol production.

Materials and methods

Microorganism, inoculum preparation, and cultivation

A yeast strain *C. tropicalis* TISTR 5306 was procured from Thailand Institute of Scientific and Technological Research (TISTR). It was maintained on Yeast-Malt (YM) agar (10 g/L of glucose, 3 g/L of yeast extract, 3 g/L of malt extract, 5 g/L of peptone, and 15 g/L of agar) with regular transfer to fresh plates every 2 weeks. For inoculum preparation, one loop full of cells from a freshly sub-cultured plate were inoculated into Erlenmeyer flask (250 mL) containing YM medium with a working volume of 100 mL. The inoculated flasks were incubated for 24 h in a rotary shaker at 30 °C with agitation set at 200 rpm. The initial cell concentration was 1.23×10^9 CFU/mL with cell viability above 99%.

Corncob hemicellulosic hydrolysate preparation

Corncob was selected as raw material as our previous study on optimization of the pretreatment evident that the highest sugar conversions were obtained from corncob followed by the rice straw and sugarcane bagasse¹⁶.

Corncoobs were purchased from Chiang Mai Provincial Livestock office in Thailand. The structural composition of corncob was determined on dry basis as follows (w/w): 34.9 cellulose; 38.3 hemicellulose; 7.80 lignin; 19.0 extractives¹⁶. The collected corncobs were dried at 60 °C to a constant weight, then milled and sieved to isolate particles <2 mm in size. Sequential corncob pretreatment was conducted for 113 min at 95 °C using diluted sulfuric acid (H₂SO₄) (3.36% w/v) with solid corncob loading of 10% (w/v) in an autoclave¹⁶. After cooling, the liquid fraction was obtained through filtration, known as corncob hemicellulosic hydrolysate, which primarily consists of hemicellulosic sugars. The composition of the corncob hemicellulosic hydrolysate was as follows (g/L): 9.85, xylose; 0.52, glucose; 3.42 acetic acid; 0.14 furfural; 0.32 hydroxymethyl furfural (HMF); 0.86 total phenolics. Thereafter, the hydrolysate was concentrated to xylose concentration of 100 g/L using vacuum rotavapor (Greatwall, Model No. Rotavapor R-1010, China), maintaining at 100 mbar and 70 °C for the media preparation during the hydrolysate experiment. The initial volume and concentration of xylose of the original hydrolysate were used as preliminary guides to determine final volume of hydrolysate that must be attained after evaporation so that 100 g/L concentrated hydrolysate could be eventually confirmed with high performance liquid chromatography (HPLC). The composition of concentrated hydrolysate was as follows (g/L): 100, xylose; 5.45, glucose; 8.05, acetic acid; 0.08, furfural; 0.33, HMF; 8.28, total phenolics.

Xylitol production from pure sugars

Xylitol production using co-substrate cultivation was conducted in 250 mL Erlenmeyer flasks with 100 mL of working volume. Erlenmeyer flasks were incubated at 30 °C and 200 rpm in a shaking incubator with an initial pH of 6.0 under microaerobic conditions. The pure sugars media were prepared at the initial xylose + glucose concentration levels of 10 + 1, 20 + 2, 30 + 3, 40 + 4, 50 + 5, 60 + 6, 70 + 7, 80 + 8, 90 + 9, and 100 + 10 g/L. Subsequent dilution of each medium using active inoculum 10% (v/v) in logarithmic stage at 24 h, during which the initial xylose in inoculum medium was depleted, resulted in the decrease of initial sugars concentration to 9 + 0.9, 18 + 1.8, 27 + 2.7, 36 + 3.6, 45 + 4.5, 54 + 5.4, 63 + 6.3, 72 + 7.2, 81 + 8.1, and 90 + 9.0 g/L. The ratio of xylose and glucose in each medium was thus still maintained initially at 10:1 when the yeast began to propagate. Experiments for model development were performed with the xylose + glucose concentrations of 18 + 1.8, 36 + 3.6, 54 + 5.4, 72 + 7.2, and 90 + 9.0 g/L. Interpolation validation was conducted with the xylose + glucose concentrations of 27 + 2.7, 45 + 4.5, 63 + 6.3, and 81 + 8.1 g/L. Extrapolation validations was conducted with the xylose + glucose concentrations of 9 + 0.9 g/L. Each experiment was performed in quintuplicate. Samples were taken at a regular interval of 12 h until 48 h and then every 24 h until the cessation of cultivation time of 168 h to measure the concentrations of xylose, glucose, xylitol, and dried biomass.

Xylitol production from non-detoxified corncob hemicellulosic hydrolysate

Xylitol production using non-detoxified corncob hemicellulosic hydrolysate was conducted under identical conditions as the experiment using pure sugars. In the case of sugars concentration, xylose and glucose were adjusted by diluting concentrated hydrolysate accordingly and then adding additional pure glucose to achieve a xylose and glucose ratio of 10:1. The pH of the hydrolysate was adjusted to 6.0 by adding either 5 M NaOH or 5 M HCl. The effects of non-detoxified hydrolysate on substrate utilization, biomass, and xylitol production were evaluated by comparing with pure sugars experiment. The predictability of developed model was assessed in the hydrolysate experiment by comparing the experimental data with the kinetic profiles of microbial growth, sugars consumption, and xylitol production. Samples were taken at a regular interval of 12 h until 48 h and then every 24 h until the cessation of cultivation time of 168 h to measure the concentrations of xylose, glucose, xylitol, and dried biomass.

Model development

Rate equations are crucial to model development as they establish a quantitative framework for comprehending the process. In this study, the foundation for rate equations was derived from previous models developed for *C. shehatae* ATCC 22,984¹⁷ and *Zymomonas mobilis* ZM4 (PzB5)¹⁸ cultivation using mixture of xylose and glucose. The model assumes that the predominating factors influencing kinetics are substrate and product inhibition with both a threshold level. Additionally, the substrate limitation effect from Monod-type expressions was also integrated into the model. Simulation profiles were generated using numerical integration with the Euler-Cauchy method and a time increment (Δt) of 0.2 h.

In the co-substrate cultivation by *C. tropicalis*, the consumption and growth occur simultaneously on both xylose and glucose¹⁹. Although *C. tropicalis* possesses specific transport proteins or transporters that are responsible for the uptake of xylose and glucose, the presence of one sugar invariably affects the uptake of the other. Therefore, sugar uptake and growth are represented by the maximum consumption rate and the maximum specific growth rate, respectively, on xylose and glucose as single carbon sources. The proportioning factors for xylose (α) and glucose ($1 - \alpha$) were applied to describe their consumptions and contributions to biomass formation. Considering this, the equations representing microbial growth were given in Eqs. (1), (2), and (3). The xylose and glucose uptake can be represented by Eqs. (4) and (5), respectively.

Microbial growth rate:

$$\frac{dx}{dt} = [\alpha r_{x,1} + (1 - \alpha) r_{x,2}] x \quad (1)$$

$$r_{x,1} = \mu_{\max,1} \left(\frac{S}{K_{s,x,1} + S_1} \right) \left(1 - \frac{P - P_{i,x,1}}{P_{m,x,1} - P_{i,x,1}} \right) \left(\frac{K_{i,x,1}}{K_{i,x,1} + S_1} \right) \quad (2)$$

$$r_{x,2} = \mu_{\max,2} \left(\frac{S}{K_{sx,2} + S_2} \right) \left(1 - \frac{P - P_{ix,2}}{P_{mx,2} - P_{ix,2}} \right) \left(\frac{K_{ix,2}}{K_{ix,2} + S_2} \right) \quad (3)$$

Xylose (S_1) and Glucose (S_2) uptake rate:

$$\frac{dS_1}{dt} = -\alpha q_{s\max,1} \left(\frac{S_1}{K_{ss,1} + S_1} \right) \left(1 - \frac{P - P_{is,1}}{P_{ms,1} - P_{is,1}} \right) \left(\frac{K_{is,1}}{K_{is,1} + S_1} \right) x \quad (4)$$

$$\frac{dS_2}{dt} = -(1 - \alpha) q_{s\max,2} \left(\frac{S_2}{K_{ss,2} + S_2} \right) \left(1 - \frac{P - P_{is,2}}{P_{ms,2} - P_{is,2}} \right) \left(\frac{K_{is,2}}{K_{is,2} + S_2} \right) x \quad (5)$$

Kim et al.²⁰ reported that in co-substrate cultivation using *C. tropicalis* ATCC 13,803 cultivated in xylose and glucose concentrations of 100 g/L and 20 g/L, respectively, only ethanol was produced as a by-product. Silva et al.²¹ found that the rise of glucose/xylose ratio of 1:2.5 resulted in the elevated by-products formation using *C. guiliermondii* FTI 20,037. Therefore, to simplify the model, the side reactions were neglected, and xylitol was assumed as the only product from xylose. The xylitol production rate can be represented by Eq. (6).

Xylitol (P) production rate:

$$\frac{dP}{dt} = q_{p,\max} \left(\frac{S_1}{K_{sp} + S_1} \right) \left(1 - \frac{P - P_{ip}}{P_{mp} - P_{ip}} \right) \left(\frac{K_{ip}}{K_{ip} + S_1} \right) x \quad (6)$$

The terms with subscript 1 referring to xylose and subscript 2 referring to glucose.

Parameters estimation and optimization

Model parameters estimation was performed according to a previously described program written in Microsoft EXCEL using Visual Basic for Applications (VBA)^{17,18,22,23}. The optimal parameters for each equation were determined by minimizing the total residual sum of squares (RSS_{total}) between the experimental data and predicted profiles from five batches of cultivation with xylose + glucose concentrations of 18 + 1.8, 36 + 3.6, 54 + 5.4, 7.2 + 7.2, and 90 + 9.0 g/L.

The RSS for each batch cultivation was defined in Eq. (7):

$$RSS_{total} = RSS_x + RSS_{s_1} + RSS_{s_2} + RSS_p \quad (7)$$

where x , S_1 , S_2 , and P are the dried biomass concentration, xylose concentration, glucose concentration, and xylitol concentration, respectively. RSS_x , RSS_{s_1} , RSS_{s_2} , and RSS_p represent the residual sum of squares for each respective variable. RSS_{total} was used as the objective function, while the total mean square (MS_{total}) and the correlation coefficient (R^2) were calculated simultaneously. The statistical parameters (RSS_{total} , MS_{total} , R^2) were employed to evaluate the quality of fit²³.

Analytical methods

Cell viability of yeast was measured using a microscope (CX23, Olympus, Tokyo, Japan) with a hemocytometer¹⁶. Dried biomass concentration was obtained through the method of weight difference using the harvested cells from cultivation broth by centrifugation at $2,822 \times g$ for 10 min. The cells were washed twice with distilled water, followed by drying at 105 °C until steady weight. The concentrations of glucose, xylose, and xylitol were quantified by HPLC with Aminex® HPX-87H column (Bio-Rad, USA). The concentrations of acetic acid, furfural, and HMF in the corncob hemicellulosic hydrolysate were quantified using a ZORBAX Eclipse XDB-C18 column (Agilent Technologies, USA)²⁴. The total concentrations of phenolic compounds were estimated by spectrophotometry using Folin-Ciocalteu reagent (Sigma, USA)²⁵.

Statistical analysis

The analyses were reported as mean \pm standard error (SE) and conducted with Statistical Packages for the Social Sciences (SPSS, version 17.0) using one-way analyses of variance (ANOVA). Statistical differences among means were determined using Duncan's multiple comparisons and considered significant at $p \leq 0.05$ ^{26,27}.

Xylitol yield and productivity were calculated in Eqs. (8) and (9):

$$\text{Xylitol yield (g/g)} = \frac{\text{produced xylitol concentration (g/L)}}{\text{consumed xylose (g/L)}} \quad (8)$$

$$\text{Xylitol productivity (g/L/h)} = \frac{\text{produced xylitol concentration (g/L)}}{\text{cultivation time (h)}} \quad (9)$$

Results and discussion

Effects of substrate concentration on biomass and xylitol production

Ten batch bioconversions using *C. tropicalis* cultivated in co-substrate of xylose and glucose with different concentrations of xylose (10 - 100 g/L) under a ratio of 10:1 were assessed. The experimental data of fermentative parameters are tabulated in Table 1. Both the mitigation of $Y_{x/s}$ and Q_x as well as the increment of Y_{p/s_1} and Q_p incorporated with increased $Y_{p/x}$ could signify that the desired metabolic pathway of converting xylose to xylitol instead of biomass was achieved under the condition of relatively high substrate concentrations. As a result of

Exp	$S_1 + S_2$ (g/L)	Time (h)	P_{max} (g/L)	x (g/L)	$Y_{p/s1}^a$ (g/g)	$Y_{x/s1}^a$ (g/g)	$Y_{p/x}^c$ (g/g)	Q_p^b (g/L/h)	Q_x^b (g/L/h)
1	9 + 0.9	48	3.38 ± 0.05 ⁱ	4.21 ± 0.09 ^f	0.38 ± 0.01 ^h	0.43 ± 0.01^a	0.79 ± 0.01 ⁱ	0.07 ± < 0.01 ^j	0.09 ± < 0.01 ^j
2	18 + 1.8	48	8.91 ± 0.02 ⁱ	6.24 ± 0.24 ^e	0.50 ± < 0.01 ^g	0.36 ± 0.01 ^b	1.36 ± 0.03 ^h	0.19 ± 0.00 ⁱ	0.14 ± < 0.01 ^b
3	27 + 2.7	48	15.7 ± 0.04 ^h	6.96 ± 0.05 ^{de}	0.58 ± < 0.01 ^f	0.26 ± < 0.01 ^c	2.27 ± 0.01 ^g	0.33 ± < 0.01 ^h	0.14 ± < 0.01^a
4	36 + 3.6	48	23.6 ± 0.07 ^g	6.55 ± 0.03 ^e	0.65 ± < 0.01 ^{cd}	0.18 ± 0.01 ^d	3.59 ± 0.01 ^f	0.49 ± < 0.01 ^g	0.14 ± < 0.01 ^{ab}
5	45 + 4.5	72	27.8 ± 0.25 ^f	8.09 ± 0.25 ^{cd}	0.62 ± < 0.01 ^e	0.18 ± 0.04 ^{de}	3.47 ± 0.09 ^{ef}	0.39 ± < 0.01 ^f	0.11 ± < 0.01 ^{cde}
6	54 + 5.4	72	33.7 ± 0.26 ^e	8.78 ± 0.35^a	0.62 ± 0.01 ^{de}	0.16 ± 0.01 ^e	3.89 ± 0.14 ^e	0.47 ± 0.01 ^e	0.12 ± < 0.01 ^c
7	63 + 6.3	72	40.0 ± 0.29 ^d	8.59 ± 0.14 ^{ab}	0.63 ± 0.02 ^e	0.14 ± < 0.01 ^f	4.61 ± 0.06 ^d	0.55 ± < 0.01 ^d	0.12 ± < 0.01 ^{cd}
8	72 + 7.2	72	48.7 ± 0.18 ^c	7.66 ± 0.05 ^{cd}	0.68 ± 0.01 ^{bc}	0.11 ± < 0.01 ^g	6.35 ± 0.06 ^c	0.68 ± 0.01 ^c	0.11 ± < 0.01 ^{ef}
9	81 + 8.1	72	57.2 ± 0.23 ^b	7.92 ± 0.18 ^{bc}	0.71 ± 0.01 ^b	0.10 ± < 0.01 ^{gh}	7.27 ± 0.17 ^b	0.79 ± 0.01 ^b	0.11 ± < 0.01 ^{de}
10	90 + 9.0	72	64.5 ± 0.32^a	7.20 ± 0.06 ^{cde}	0.78 ± < 0.01^a	0.09 ± < 0.01 ⁱ	8.79 ± 0.07^a	0.90 ± < 0.01^a	0.10 ± < 0.01 ^f

Table 1. Maximum xylitol concentration and its corresponding time and dried biomass concentration being produced as well as associated experimental kinetic parameters after cultivation with different xylose + glucose initial concentration levels maintained at 10:1 ratio. S_1 is the xylose concentration (g/L); S_2 is the glucose concentration (g/L); P_{max} is the maximum xylitol concentration (g/L); x is the dried biomass concentration at maximum xylitol concentration (g/L). The values indicate the mean value ± standard error (SE). ^aMass yield is calculated from the ratio of total concentration of produced xylitol or dried biomass per total consumed xylose. ^bVolumetric productivity is calculated from the ratio of total concentration of produced xylitol or dried biomass per total production time. ^cMass yield is calculated from the ratio of total concentration of produced xylitol per total produced dried biomass.

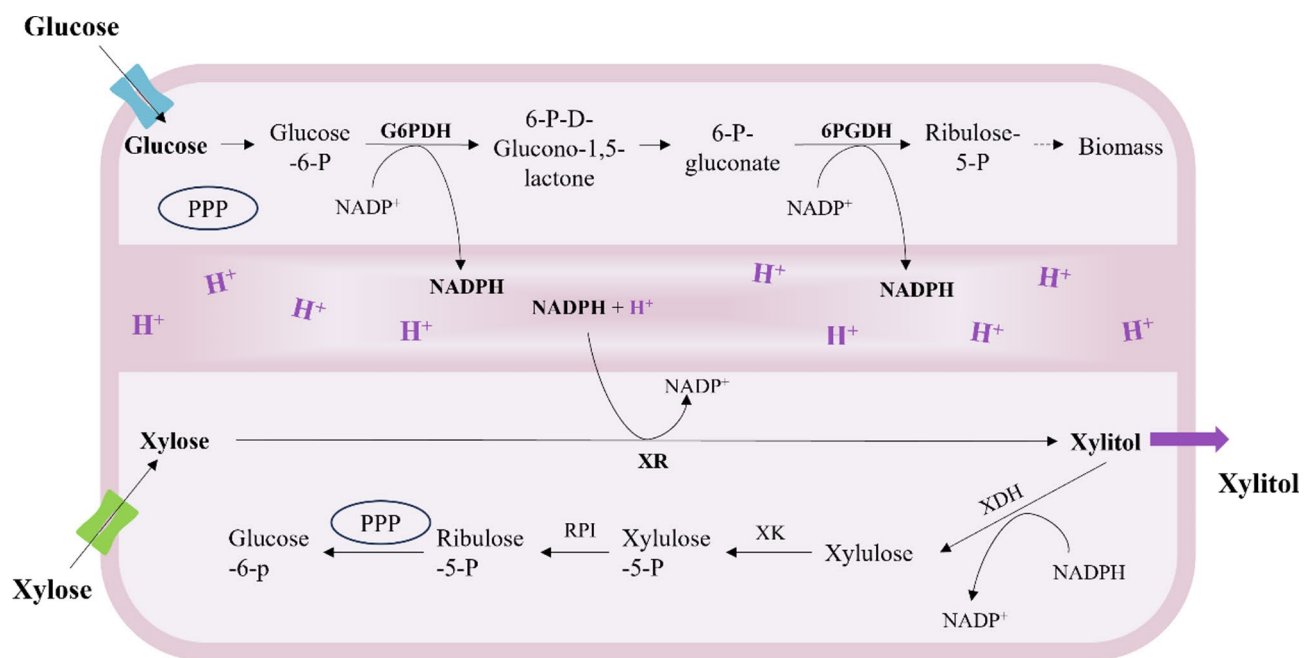


Fig. 1. Co-substrate xylitol production at a low level of glucose.

it, although the increment of the initial substrate concentrations caused a longer cultivation time, the lowest biomass yield of 0.09 g/g incorporated with the highest xylitol concentration, yield, and productivity of 64.5 g/L, 0.78 g/g, and 0.90 g/L/h, respectively, were achieved by using xylose concentration of 90 g/L with additional 9.0 g/L glucose (Table 1). It can be concluded that the higher xylose concentration benefits the decrease of the fraction of xylose metabolized to generate biomass and increase the conversion efficiencies of xylose to xylitol. This phenomenon can be explained by a trade-off between xylitol production and biomass formation. As shown in Fig. 1, xylitol is directly converted from xylose, whereas the biomass formation from xylose needs through XDH followed by xylulokinase (XK) enzymatic reactions. XDH converts xylitol back to xylulose and XK phosphorylates xylulose to xylulose-5-phosphate (Xylulose-5-P), a pivotal step in xylose metabolism. Xylulose-5-P is an intermediate that can feed directly into the PPP by ribose-5-phosphate isomerase (RPI). The higher xylitol productivity was the result of a higher XR:XDH ratio²⁸.

Additionally, the low level of glucose supports the conversion of xylose into xylitol. Xylose is directly converted into xylitol by XR in the presence of coenzyme, namely, nicotinamide adenine dinucleotide phosphate

(NADPH) or nicotinamide adenine dinucleotide (NADH). NADPH coupling oxidation assay for XR revealed that wild type *C. tropicalis* exhibited higher specific XR activity when cofactored with NADPH rather than NADH by 7.8 times³⁵. Continuous NADPH regeneration is a necessity in an efficient xylitol production system through the pentose phosphate pathway (PPP) with enzymatic coupling reduction processes of glucose-6-phosphate dehydrogenase (G6PDH) and 6-phosphogluconate dehydrogenase (6PGDH)²⁰. The PPP is primarily an anabolic pathway that utilizes the C6 sugars of glucose to generate C5 sugars and reducing equivalents. The preference for using glucose as a carbon and energy source arises from its ease of metabolism and efficient energy extraction properties. The presence of a lower level of glucose could enhance NADPH supplement and further benefits xylitol production³. On the other hand, a low level of glucose can also enhance the secretion of extracellular xylitol as less of the xylitol formed is oxidized into xylulose by xylitol dehydrogenase (XDH) with NAD⁺ as an electron acceptor. The presence of glucose can hinder further oxidation by slowing down the glucose-6-phosphate (Glucose-6-P) production from xylulose via xylulose-5-phosphate (Xylulose-5-P)⁸. Consequently, the higher xylitol concentration could be achieved by the high fraction of xylose metabolized to xylitol and additional low level of glucose via enhancing NADPH supplement and decreasing xylitol oxidation. Since the highest xylitol yield and productivity were achieved by using xylose + glucose concentrations of 90 + 9.0 g/L, the subsequent hydrolysate experiment was performed with these initial values.

Our results are comparable to Saha et al.²⁹, where they have subjected the *Barnettozyma populi* NRRL Y-12728 for xylitol production using xylose concentrations from 50 to 75 and 100 g/L. The yeast strain produced 32.2, 49.9, and 58.1 g/L xylitol with a yield of 0.65, 0.70, and 0.71 g/g and productivities of 0.45, 0.52, and 0.43 g/L/h at 50, 75, and 100 g/L xylose, respectively. Eryasar and Karasu-Yalcin³⁰ investigated strains of *C. tropicalis*, *C. famata*, *C. guilliermondii*, and *D. hansenii* for xylitol production, the highest xylitol concentrations of 83.28 and 54.07 g/L from 100 g/L xylose were achieved by using *C. tropicalis* M2 and *C. tropicalis* M43, respectively. Prakash et al.³¹ reported that maximum xylitol production of 68.6 g/L from 100 g/L of xylose with a yield of 0.76 g/g and volumetric productivity of 0.44 g/L/h were achieved by using *D. hansenii*. Xu et al.³² reported that the accumulation of xylitol reached the maximum at an initial xylose concentration of 100 g/L (65.8 g/L) and then decreased when the initial xylose concentration exceeded 100 g/L using *C. tropicalis* 31,949. *C. tropicalis* is a promising strain for xylitol production, the higher yield of 0.78 g/g and productivity of 0.90 g/L/h in this study may be attributed to the additional glucose.

Model development and searched parameters assessment

Five batch cultivations with initial xylose (S_1) and glucose (S_2) concentrations of 18 + 1.8, 36 + 3.6, 54 + 5.4, 72 + 7.2, and 90 + 9.0 g/L have been conducted and used in the estimation of parameters in a complete model through the parameter searching program. The optimal parameter constants are presented in Table 2, while the parameter values of maximum specific utilization rate of xylose ($q_{smax,1}$) and glucose ($q_{smax,2}$) as well as maximum specific production rate (q_{pmax}) were functionally associated with their corresponding initial sugars concentration (Fig. 2). As can be seen from Fig. 2(A), $q_{smax,1}/q_{smax,2}$ was decreased with S_2 up to 5 g/L after which a plateau was reached at ~0.4 with R^2 of 0.996. The relationship between q_{pmax} and S_1 as shown in Fig. 2(B) with R^2 of 0.998.

The $q_{smax,1}$ was restricted by critical xylose concentration ($S_{1,crit}$) as presented in Eq. (10). The relationships between $q_{smax,1}/q_{smax,2}$ with S_2 and q_{pmax} with S_1 were fitted to the polynomial equations as shown in Eqs. (11) and (12), respectively.

$$q_{smax,1} = \begin{cases} 7.397 \times 10^{-3} S_1 + 0.4551; S_1 < S_{1,crit} \\ q_{smax,1,crit}; S_1 \geq S_{1,crit} \end{cases} \quad (10)$$

$$\frac{q_{smax,1}}{q_{smax,2}} = -4.702 \times 10^{-2} S_2^3 + 8.889 \times 10^{-1} S_2^2 - 5.47 S_2 + 1.171 \quad (11)$$

$$q_{pmax} = 1.972 \times 10^{-6} S_1^3 - 3.425 \times 10^{-4} S_1^2 + 2.112 \times 10^{-2} S_1 - 8.559 \times 10^{-2} \quad (12)$$

The simulation curves from the model are depicted in Fig. 3 (B, D, F, H, J) alongside experimental data points for comparison. As evident from Fig. 3 (B, D, F, H, J) and Table 3 (Parameter search) with average RSS_{total} , R^2 , and MS_{total} values of 192, 0.982, and 12.8, respectively, the model demonstrated an acceptable fitting of the data within the xylose concentration range of 20 - 100 g/L.

Model validation using optimized parameters

Model validation was carried out by employing the developed model and optimized kinetic parameters to simulate profiles of sugars consumption, biomass, and xylitol production. These simulated profiles were subsequently compared to actual experimental data or expected trends to evaluate the accuracy and effectiveness of the model. Interpolation and extrapolation validations were performed by applying the model to different experimental sets with initial xylose concentrations within and outside of the range of 20 - 100 g/L. Interpolation test was preformed using sets of xylose + glucose concentrations of 27 + 2.7, 45 + 4.5, 63 + 6.3, and 81 + 8.1 g/L. The extrapolation test was performed using 9 + 0.9 g/L. As evident from the simulation profiles shown in Fig. 3 (A, C, E, G, I) and Table 3 (Validation) with average RSS_{total} , R^2 , and MS_{total} values of 132, 0.975, and 8.81, respectively, it provided credible evidence that the model could accurately predict experimental results within the xylose concentration range of 10 - 100 g/L under a xylose and glucose ratio of 10:1.

Equations	Parameters	Values	Units
Substrate uptake	$K_{ss,1}$	2.04	g/L
	$K_{ss,2}$	0.18	g/L
	$P_{is,1}$	10.4	g/L
	$P_{is,2}$	12.4	g/L
	$P_{ms,1}$	228	g/L
	$P_{ms,2}$	30.2	g/L
	$K_{is,1}$	600	g/L
	$K_{is,2}$	600	g/L
	$S_{l,crit}$	59.5	g/L
	$q_{smax1,crit}$	0.90	g/g/L
Microbial growth	$\mu_{max,1}$	0.16	h ⁻¹
	$\mu_{max,2}$	0.03	h ⁻¹
	α	0.59	-
	β	0.41	-
	$K_{sx,1}$	1.35	g/L
	$K_{sx,2}$	0.19	g/L
	$P_{ix,1}$	14.0	g/L
	$P_{ix,2}$	47.9	g/L
	$P_{mx,1}$	149	g/L
	$P_{mx,2}$	320	g/L
	$K_{ix,1}$	95.0	g/L
	$K_{ix,2}$	151	g/L
Xylitol production	K_{sp}	4.25	g/L
	P_{ip}	11.3	g/L
	P_{mp}	111	g/L
	K_{ip}	254	g/L

Table 2. Optimal kinetic parameters for all data sets.

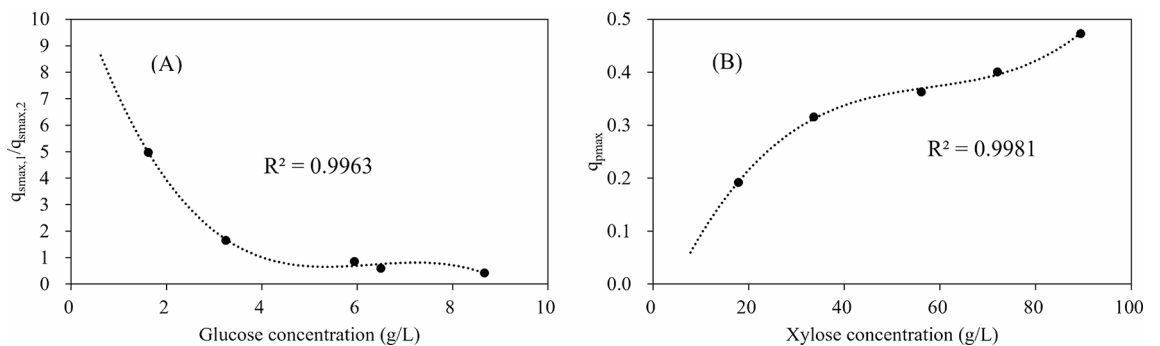


Fig. 2. The relationships between variables of the maximum specific xylose utilization rate ($q_{smax,1}$), maximum specific glucose utilization rate ($q_{smax,2}$), and maximum specific xylitol production rate (q_{pmax}) with their corresponding sugars concentration. (A) relationship between $q_{smax,1}/q_{smax,2}$ with glucose concentration, (B) relationship between q_{pmax} with xylose concentration.

Optimal kinetic parameters

Optimal kinetic parameters for substrate uptake, biomass production, and xylitol production are shown in Table 2. The proportioning factors represent the relative preference for sugars utilization and biomass production from either xylose or glucose. The factors for xylose ($\alpha=0.59$) and glucose ($1 - \alpha=0.41$) indicated that the specific xylose uptake was 59% of its maximum value, while that of glucose was 41% of its maximum when the two sugars were presented initially in a 10:1 ratio. The maximum specific growth rate (μ_{max}) represents metabolism or substrate utilization, which is attributed to transport of substrate across the cells membrane, the faster flux is therefore required to achieve high μ_{max} ¹⁵. In the present model, μ_{max} on xylose ($\mu_{max,1}$) was approximately 5 times that of glucose ($\mu_{max,2}$). It indicated that the yeast grew faster and was more efficient at utilizing xylose compared to glucose. This may be related to the two sugars transporter proteins - CtStp 1 and CtStp2 in *C. tropicalis*. Growth curve and sugars consumption profiles revealed uptake of both glucose and xylose simultaneously. However, the

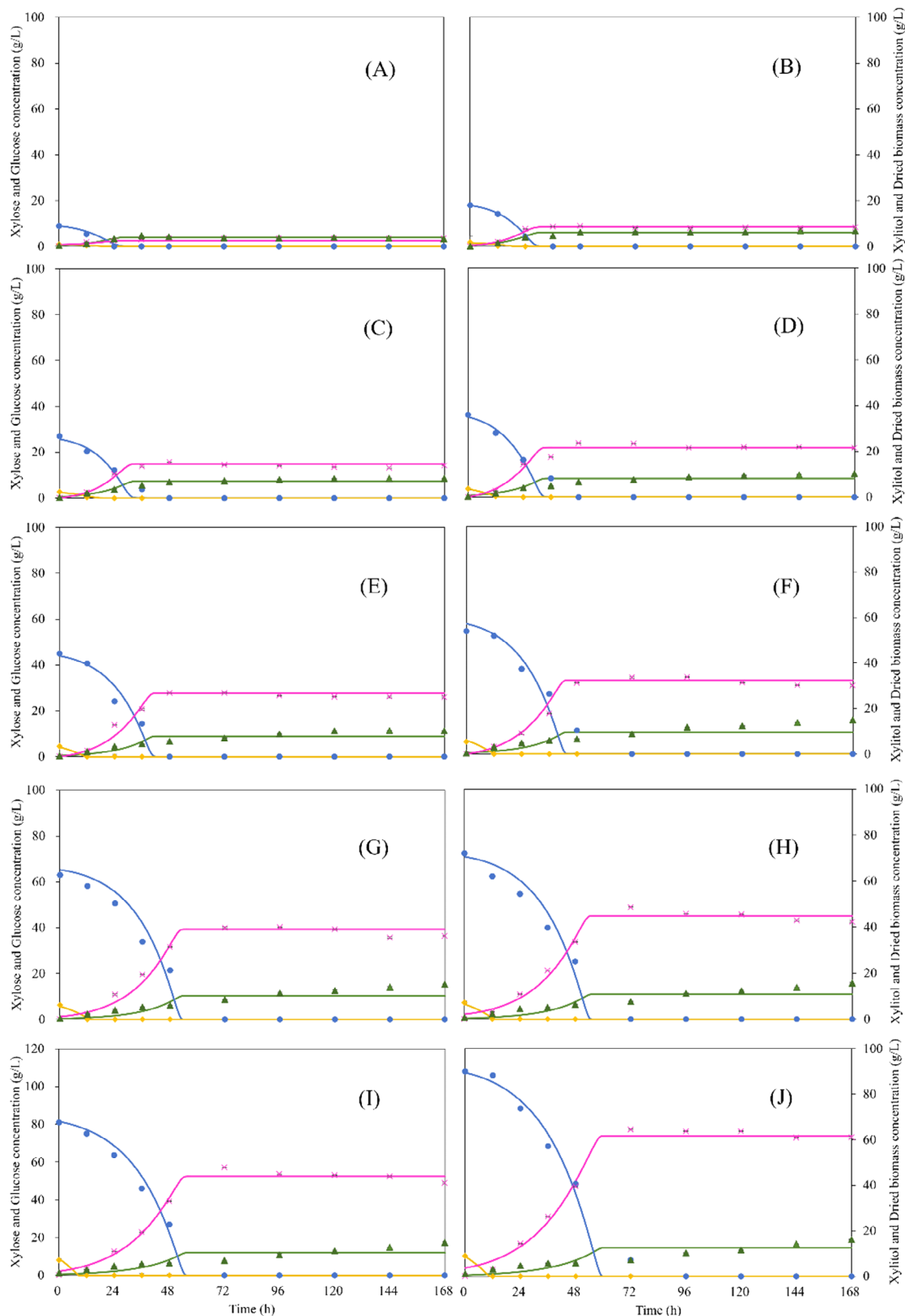


Fig. 3. Simulation (line) and experimental (point) data for batch xylitol production by *C. tropicalis* using xylose and glucose as substrate (g/L): (A) 10 xylose + 1 glucose, (B) 20 xylose + 2 glucose, (C) 30 xylose + 3 glucose, (D) 40 xylose + 4 glucose, (E) 50 xylose + 5 glucose, (F) 60 xylose + 6 glucose, (G) 70 xylose + 7 glucose, (H) 80 xylose + 8 glucose, (I) 90 xylose + 9 glucose, and (J) 100 xylose + 10 glucose. Representations: blue (xylose); yellow (glucose); pink (xylitol); green (dried biomass). The graph represents the mean value \pm standard error (SE) values.

Sections	$S_1 + S_2$ (g/L)	RSS_{total}	R^2	MS_{total}
Parameter search	18 + 1.8	5.80	0.994	0.39
	36 + 3.6	120	0.972	7.99
	54 + 5.4	341	0.965	22.8
	72 + 7.2	248	0.987	16.5
	90 + 9.0	245	0.993	16.3
Validation (interpolation)	27 + 2.7	38.5	0.982	2.57
	45 + 4.5	123	0.978	8.20
	63 + 6.3	274	0.982	18.3
	81 + 8.1	214	0.992	14.3
Validation (extrapolation)	9 + 0.9	10.4	0.942	0.69

Table 3. Summary of related statistical parameters used in fitting quality assessment between the predicted profiles and pure sugars experimental data. S_1 is the xylose concentration (g/L); S_2 is the glucose concentration (g/L); RSS_{total} is the total residual sum of squares, R^2 is the correlation coefficient, MS_{total} is the total mean square.

CtStp1 showed relatively less effect of glucose repression in mixed sugars and was a better transporter of xylose than CtStp2³⁴. The substrate affinity constant or Monod saturation constant (K_s) is a parameter to describe the affinity of microorganism for its substrate. It represents the substrate concentration at which half of the maximum specific growth rate was achieved. K_s associated with xylose utilization ($K_{ss,1}$) was approximately 11 times that of glucose ($K_{ss,2}$) and K_s associated with cells growth (K_{sx}) from xylose ($K_{sx,1}$) was approximately 7 times that of glucose ($K_{sx,2}$) indicating a high affinity for glucose than xylose³⁵. As shown in Eqs. (2) - (5), the substrate limitation effect on xylose utilization ($S_1/(K_{ss,1} + S_1)$) was higher than on glucose ($S_2/(K_{ss,2} + S_2)$), whereas the effect of glucose limitation ($S_2/(K_{sx,2} + S_2)$) on growth was higher than that of xylose ($S_1/(K_{sx,1} + S_1)$). This could be a possible consequence of the preference not solely relied on facilitated diffusion but also on the cellular metabolic demand and the concentration gradient of the sugars in which xylose is the major substrate for xylitol production and glucose is served for cells growth. Additionally, K_s associated with xylitol production (K_{sp}) was 4.25 g/L. The xylose limitation effect on xylitol production ($S_1/(K_{sp} + S_1)$) indicated that a relatively higher level of xylose is required to drive xylose metabolism. This requirement can be explained from the conformation of structure of XR enzyme which contains a hydrophobic binding pocket whereas xylose exhibits significant hydrophilic characteristics⁶.

Generally, high xylitol production is achieved by using high substrate concentration. However, a decrease in xylitol yield was observed when the xylose concentration increased from 75 g/L to over 100 g/L, even though *C. tropicalis* is considered an osmotolerant yeast³⁶. The substrate inhibitory constant (K_i) is a parameter used to describe the inhibitory effect of substrate on cells growth (K_{ix}) and xylitol production (K_{ip}). The constants of xylose ($K_{ix,1}$) and glucose ($K_{ix,2}$) associated with growth were 95.0 and 151 g/L, respectively. The constant of xylose associated with xylitol production (K_{ip}) was 254 g/L. As shown in Eqs. (2) and (6), the factors of $K_{ix,1}/(K_{ix,1} + S_1)$ and $K_{ip}/(K_{ip} + S_1)$ indicated that the growth was more sensitively affected by xylose concentration compared to xylitol production. Similar phenomenon was observed with xylose concentration over 200 g/L, the production of xylitol declined whereas the growth was inhibited³⁷. This may be due to the yeast possessing metabolic pathways that can convert xylose into xylitol through enzymatic reactions which can be independent to active cells division or growth process.

During cultivation, the effects from xylitol concentration (P) occurred simultaneously. The rates of cells growth on xylose ($r_{x,1}$), xylose utilization (ds_1/dt), and xylitol production (dp/dt) were promoted when P was below the threshold levels of 14.0 g/L ($P_{ix,1}$), 10.4 g/L ($P_{is,1}$), and 11.3 g/L (P_{ip}), respectively. A linear depreciate occurred when P was between the threshold and inhibitory levels, until the inhibitory effect occurred at the $P = 149$ g/L ($P_{mx,1}$), 228 g/L ($P_{ms,1}$), and 111 g/L (P_{mp}), respectively. This phenomenon can be explained by low levels of xylitol simulating XR²⁸, whereas high levels of xylitol inhibit the XR reaction³⁸. Theoretically, the factors $1 - (P - P_{ix,1})/(P_{mx,1} - P_{ix,1})$, $1 - (P - P_{is,1})/(P_{ms,1} - P_{is,1})$, and $1 - (P - P_{ip})/(P_{mp} - P_{ip}) = 0$ would occur when $P = P_{mx,1}$, $P_{ms,1}$, and P_{mp} , respectively (Eqs. 2, 4, and 6), which indicated that the growth, consumption, and production were completely stopped by xylitol. However, this was not the case as xylose has been consumed to a certain level before P reaches inhibitory levels in a batch cultivation system. The slowdown and eventual cessation of growth as well as xylitol production, especially in the cases of pure sugars cultivation, were thus principally caused by xylose limitation. This caused the values of dx/dt or dp/dt gravitated toward zero as the variable of xylose concentration was directly proportional to the growth and xylitol rate equations (Eqs. 2 and 6). It was also possible for the values of dx/dt and dp/dt to descend and finally reaching zero due to accumulated xylitol concentration ($P = P_{mx}$ or P_{mp}) in the fed-batch or continuous systems.

Model validation by extrapolation to xylitol production kinetics in hemicellulosic hydrolysate

The hydrolysate experiment was performed in batch culture system under a xylose and glucose ratio of 10:1. A lower xylitol concentration of 53.5 g/L with a yield of 0.64 g/g and productivity of 0.56 g/L/h was achieved using non-detoxified corncob hemicellulosic hydrolysate compared to pure sugars experiment. Specifically, the utilization of xylose and glucose, as well as the production of xylitol and dried biomass, were compared with pure

sugars experiment as shown in Fig. 4. Higher dried biomass production was observed for the hydrolysate after 96 h. This phenomenon may be attributed to the utilization of incompletely depleted xylose and other sugars in hydrolysate as carbon source for yeast growth. Additionally, the lower xylose consumption rate (0.91 ± 0.05 g/L/h vs. 1.13 ± 0.06 g/L/h) incorporated with lower xylitol production rate (0.64 ± 0.03 g/L/h vs. 0.97 ± 0.02 g/L/h) between 12 - 48 h and incomplete xylose utilization after 72 h were observed from hydrolysate experiment. Differences in xylose utilization and xylitol production can be associated with the presence of inhibitors in hydrolysate. Similar effects of inhibitors on xylose consumption and conversion were observed when using *C. tropicalis* for xylitol production. The inhibitors could cause mitigation in biological activities and enzymatic functions. The activity of XR enzyme regulates the flux of xylose through the metabolic pathway. Higher XR activity typically leads to faster conversion of xylose to xylitol, promoting efficient xylose consumption by microbial cells³⁹. Rafiqul et al.⁴⁰ found that acetic acid, phenolics, furfural, and HMF in hemicellulosic hydrolysate significantly inhibited XR from *C. tropicalis* IFO 0618 with concentration-50 (IC_{50}) values of 11, 6.4, 2.3, and 0.4 g/L, respectively. Kaur et al.⁴¹ reported that the addition of 2 g/L acetic acid decreased xylitol production rate by 4.18% compared to the control medium lacking inhibitor in cultivation by *C. tropicalis* OK165575. Therefore, a detoxification method is commonly employed to decrease the inhibitors concentrations and further improve the xylitol production. Kumar et al.⁴² found that 150 Da polymeric membrane was effective in removal of inhibitors from corn cob acid hydrolysate with simultaneous concentration of xylose. The removal of inhibitors like acetic acid (82.4%) and salts of acid (57.8%), respectively, and a xylitol yield of 62% were successfully achieved using *C. tropicalis* MTCC 6192. Ahuja et al.⁴³ reported that ~93.23% furfurals and 94.62% phenolics in hydrolysate were removed by using activated carbon. A xylitol yield of 0.78 g/g was achieved from the detoxified hydrolysate by *P. caribbica* MTCC 5703. The removal of furfurals and phenolics effectively improves xylitol production. Moreover, during cultivation, although *C. tropicalis* can mitigate the inhibitory effects of furfural and HMF by converting them into less toxic compounds, this process requires NAD⁺, which is also an important cofactor used in xylose metabolism^{41,44}.

The predictability of the developed model was assessed in the hydrolysate experiment by comparing the experimental data with kinetics profiles. Figure 5 depicts the simulation curves of experimental data by the developed model for prediction of sugars utilization, biomass, and xylitol production. A relatively good fit was achieved with RSS_{total} , R^2 , and MS_{total} values of 356, 0.988, and 23.8, respectively. However, these statistical parameters were lower than those for the pure sugars fitting with RSS_{total} , R^2 , and MS_{total} values of 245, 0.993, and 16.3, respectively (Table 3), due to the underprediction of dried biomass after 96 h. The good fitting of sugars utilization and xylitol production indicated that the current model also demonstrates good predictability for hydrolysate medium, whereas the underprediction of biomass production after reaching the highest xylitol concentration suggested that further modifications to the growth rate equations were necessary.

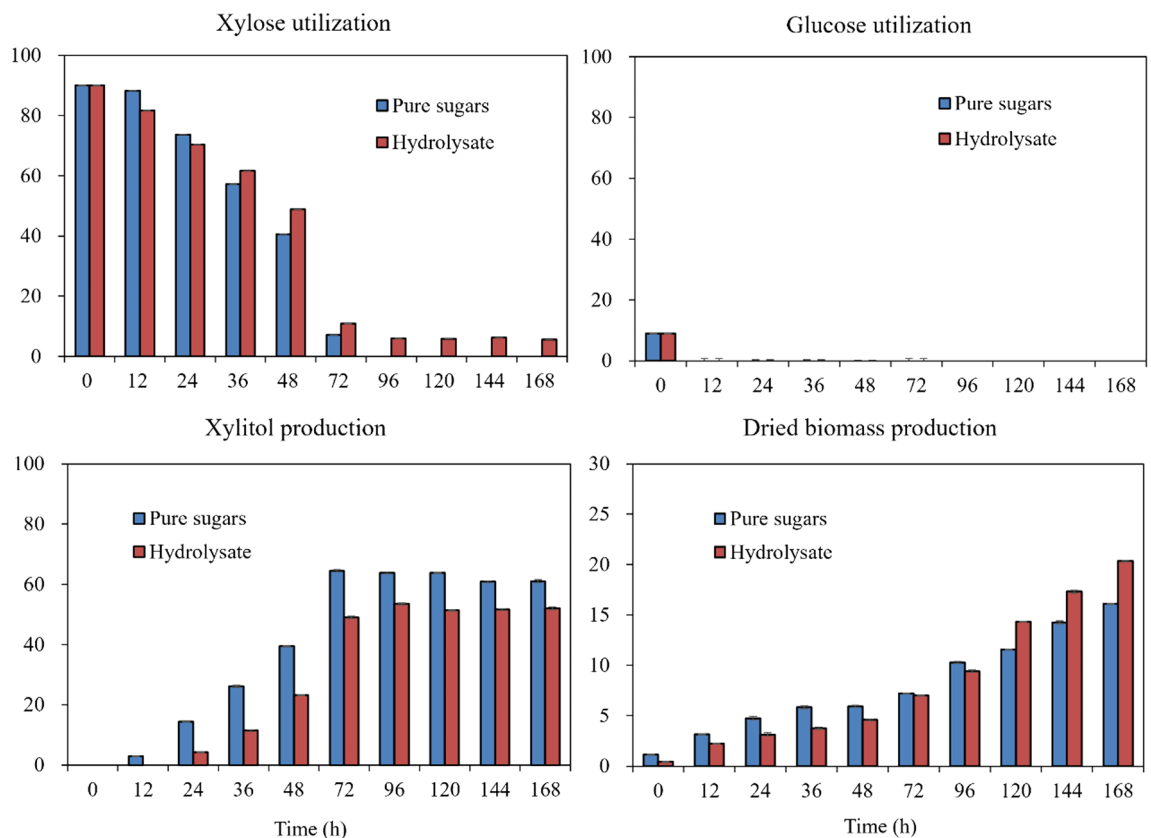


Fig. 4. Comparison of xylitol production using pure sugars and hydrolysate.

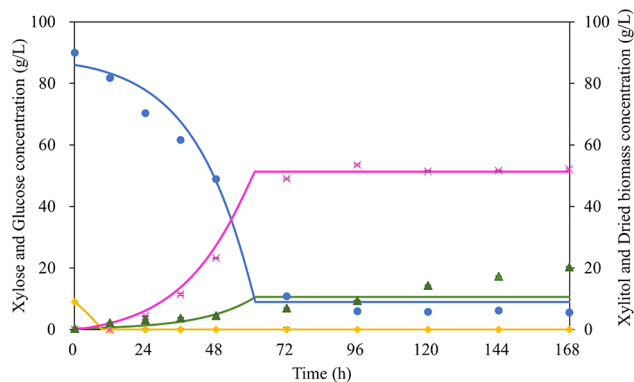


Fig. 5. Simulation (line) and experimental (point) data for batch xylitol production by *C. tropicalis* using corncob hemicellulosic hydrolysate. Representations: blue (xylose); yellow (glucose); pink (xylitol); green (dried biomass). The graph represents the mean value \pm standard error (SE) values.

Conclusion

A good agreement between simulation data and experimental results with average RSS_{total} , R^2 and MS_{total} values of 162, 0.979, and 10.8 for pure sugars as well as 368, 0.988, and 24.5 for hydrolysate, respectively, has revealed the comprehensive model development of xylitol production using *C. tropicalis* cultivated in a co-substrate of xylose (10 - 100 g/L) and glucose (1 - 10 g/L) at a ratio of 10:1. In future studies, the subsequent scaling up of current cultivation system would be important using hydrolysate in bioreactor systems with different cultivation modes, for example, batch, fed-batch, and continuous systems. The kinetic parameter estimation and model development are also important to be evaluated and compared with those values obtained from the current experiment accordingly.

Data availability

The data sets generated during and/or analysed during the current study are available from the corresponding authors on reasonable request.

Received: 30 July 2024; Accepted: 22 October 2024

Published online: 29 October 2024

References

- Witkowski, M. *et al.* Xylitol is prothrombotic and associated with cardiovascular risk. *Eur. Heart J.*, ehae244 (2024).
- Custom Market Insights (2024). Global Xylitol Market 2024 - 2032. Retrieved from <https://www.gminsights.com/industry-analysis/xylitol-market>
- Narisetty, V. *et al.* High level xylitol production by *Pichia fermentans* using non-detoxified xylose-rich sugarcane bagasse and olive pits hydrolysates. *Bioresour. Technol.* **342**, 126005 (2021).
- Feng, J. *et al.* Utilization of agricultural wastes for co-production of xylitol, ethanol, and phenylacetylcarbinol: A review. *Bioresour. Technol.*, 129926 (2023).
- Kumar, V., Binod, P., Sindhu, R., Gnansounou, E. & Ahluwalia, V. Bioconversion of pentose sugars to value added chemicals and fuels: Recent trends, challenges and possibilities. *Bioresour. Technol.* **269**, 443-451 (2018).
- Narisetty, V. *et al.* Valorisation of xylose to renewable fuels and chemicals, an essential step in augmenting the commercial viability of lignocellulosic biorefineries. *Sustain. Energy Fuels* **6**, 29-65 (2022).
- Zhang, B. *et al.* High temperature xylitol production through simultaneous co-utilization of glucose and xylose by engineered *Kluyveromyces marxianus*. *Biochem. Eng. J.* **165**, 107820 (2021).
- Tochampa, W. *et al.* A model of xylitol production by the yeast *Candida mogii*. *Bioprocess Biosyst. Eng.* **28**, 175-183 (2005).
- Wannawilai, S., Lee, W.-C., Chisti, Y. & Sirisansaneeyakul, S. Furfural and glucose can enhance conversion of xylose to xylitol by *Candida magnoliae* TISTR 5663. *J. Biotechnol.* **241**, 147-157 (2017).
- Tavares, J. M., Duarte, L. C., Amaral-Collaco, M. & Girio, F. M. The influence of hexoses addition on the fermentation of D-xylose in *Debaryomyces hansenii* under continuous cultivation. *Enzyme Microb. Technol.* **26**, 743-747 (2000).
- Sundar, M. L. & Nampoothiri, K. M. An overview of the metabolically engineered strains and innovative processes used for the value addition of biomass derived xylose to xylitol and xylonic acid. *Bioresour. Technol.* **345**, 126548 (2022).
- Mohamad, N. L., Kamal, S. M. M., Mokhtar, M. N., Husain, S. A. & Abdullah, N. Dynamic mathematical modelling of reaction kinetics for xylitol fermentation using *Candida tropicalis*. *Biochem. Eng. J.* **111**, 10-17 (2016).
- Manaf, S. F. A., Luthfi, A. A. I., Tan, J. P., Abdul, P. M. & Jamali, N. S. Kinetic study and model of fermentation parameters affected growth and xylitol production in bioreactor by *Kluyveromyces marxianus* ATCC 36,907. *Biomass Convers. Biorefin.* **13**, 7247-7263 (2023).
- Mardawati, E., Trirakhmadi, A., Kresnowati, M. & Setiadi, T. Kinetic study on fermentation of xylose for the xylitol production. *J. Ind. Inf. Technol. Agric.* **1**, 1-8 (2017).
- Tizazu, B. Z., Roy, K. & Moholkar, V. S. Ultrasonic enhancement of xylitol production from sugarcane bagasse using immobilized *Candida tropicalis* MTCC 184. *Bioresour. Technol.* **268**, 247-258 (2018).
- Porninta, K. *et al.* Pretreatment and enzymatic hydrolysis optimization of lignocellulosic biomass for ethanol, xylitol, and phenylacetylcarbinol co-production using *Candida magnoliae*. *Front. Bioeng. Biotechnol.* **11** (2023).
- Yuvadetkun, P., Leksawasdi, N. & Boonmee, M. Kinetic modeling of *Candida shehatae* ATCC 22984 on xylose and glucose for ethanol production. *Prep. Biochem. Biotechnol.* **47**, 268-275 (2017).
- Leksawasdi, N., Joachimsthal, E. L. & Rogers, P. L. Mathematical modelling of ethanol production from glucose/xylose mixtures by recombinant *Zymomonas mobilis*. *Biotechnol. Lett.* **23**, 1087-1093 (2001).

19. Chattopadhyay, A. & Maiti, M. K. Efficient xylose utilization leads to highest lipid productivity in *Candida tropicalis* SY005 among six yeast strains grown in mixed sugar medium. *Appl. Microbiol. Biotechnol.* **104**, 3133–3144 (2020).
20. Kim, J., Ryu, Y. & Seo, J. Analysis and optimization of a two-substrate fermentation for xylitol production using *Candida tropicalis*. *J. Ind. Microbiol. Biotechnol.* **22**, 181–186 (1999).
21. Silva, D. D., Mancilha, I. M., Silva, S. S. & Felipe, M. D. Improvement of biotechnological xylitol production by glucose during culture of *Candida guilliermondii* in sugarcane bagasse hydrolysate. *Brazil. Arch. Biol. Technol.* **50**, 207–215 (2007).
22. Leksawasdi, N., Breuer, M., Hauer, B., Rosche, B. & Rogers, L. Kinetics of pyruvate decarboxylase deactivation by benzaldehyde. *Biocatalysis Biotransform.* **21**, 315–320 (2003).
23. Khemacheewakul, J. et al. Validation of mathematical model with phosphate activation effect by batch (*R*)-phenylacetylcarbinol biotransformation process utilizing *Candida tropicalis* pyruvate decarboxylase in phosphate buffer. *Sci. Rep.* **11**, 1–11 (2021).
24. Nunta, R. et al. Ethanol and phenylacetylcarbinol production processes of *Candida tropicalis* TISTR 5306 and *Saccharomyces cerevisiae* TISTR 5606 in fresh juices from longan fruit of various sizes. *J. Food Process. Preserv.* **42**, e13815 (2018).
25. Lee, S. J. et al. Phenolic compounds: Strong inhibitors derived from lignocellulosic hydrolysate for 2, 3-butanediol production by *Enterobacter aerogenes*. *Biotechnol. J.* **10**, 1920–1928 (2015).
26. Mahakuntha, C., Reungsang, A., Nunta, R. & Leksawasdi, N. Kinetics of whole cells and ethanol production from *Candida tropicalis* TISTR 5306 cultivation in batch and fed-batch modes using assorted grade fresh longan juice. *Anais da Acad. Brasileira de Ciências* **93**, e20200220 (2021).
27. Khemacheewakul, J. et al. Development of mathematical model for pyruvate decarboxylase deactivation kinetics by benzaldehyde with inorganic phosphate activation effect. *Chiang Mai J. Sci.* **45**, 1426–1438 (2018).
28. Tamburini, E., Bianchini, E., Bruni, A. & Forlani, G. Cosubstrate effect on xylose reductase and xylitol dehydrogenase activity levels, and its consequence on xylitol production by *Candida tropicalis*. *Enzyme Microb. Technol.* **46**, 352–359 (2010).
29. Saha, B. C. & Kennedy, G. J. Optimization of xylitol production from xylose by a novel arabinol limited co-producing *Barnettozyma populi* NRRL Y-12728. *Prep. Biochem. Biotechnol.* **51**, 761–768 (2021).
30. Eryasar, K. & Karasu-Yalcin, S. Evaluation of some lignocellulosic byproducts of food industry for microbial xylitol production by *Candida tropicalis*. *Biotech* **6**, 1–7 (2016).
31. Prakash, G., Varma, A., Prabhune, A., Shouche, Y. & Rao, M. Microbial production of xylitol from D-xylose and sugarcane bagasse hemicellulose using newly isolated thermotolerant yeast *Debaryomyces hansenii*. *Bioresour. Technol.* **102**, 3304–3308 (2011).
32. Xu, L. et al. Xylitol production by *Candida tropicalis* 31949 from sugarcane bagasse hydrolysate. *Sugar Tech.* **21**, 341–347 (2019).
33. Kim, S., Lee, J. & Sung, B. H. Isolation and characterization of the stress-tolerant *Candida tropicalis* YHJ1 and evaluation of its xylose reductase for xylitol production from acid pre-treatment wastewater. *Front. Bioeng. Biotechnol.* **7**, 138 (2019).
34. Chattopadhyay, A., Singh, R., Das, A. K. & Maiti, M. K. Characterization of two sugar transporters responsible for efficient xylose uptake in an oleaginous yeast *Candida tropicalis* SY005. *Archiv. Biochem. Biophys.* **695**, 108645 (2020).
35. Prabhu, A. A. et al. Enhanced xylitol production using non-detoxified xylose rich pre-hydrolysate from sugarcane bagasse by newly isolated *Pichia fermentans*. *Biotechnol. Biofuels* **13**, 1–15 (2020).
36. Zhang, C., Qin, J., Dai, Y., Mu, W. & Zhang, T. Atmospheric and room temperature plasma (ARTP) mutagenesis enables xylitol over-production with yeast *Candida tropicalis*. *J. Biotechnol.* **296**, 7–13 (2019).
37. Tamburini, E., Costa, S., Marchetti, M. G. & Pedrini, P. Optimized production of xylitol from xylose using a hyper-acidophilic *Candida tropicalis*. *Biomolecules* **5**, 1979–1989 (2015).
38. Louie, T. M. et al. Production of bio-xylitol from D-xylose by an engineered *Pichia pastoris* expressing a recombinant xylose reductase did not require any auxiliary substrate as electron donor. *Microbial. Cell Factories* **20**, 1–13 (2021).
39. Sun, T., Yu, Y., Wang, K., Ledesma-Amaro, R. & Ji, X.-J. Engineering *Yarrowia lipolytica* to produce fuels and chemicals from xylose: A review. *Bioresour. Technol.* **337**, 125484 (2021).
40. Rafiqul, I., Sakinah, A. & Zularisam, A. Inhibition by toxic compounds in the hemicellulosic hydrolysates on the activity of xylose reductase from *Candida tropicalis*. *Biotechnol. Lett.* **37**, 191–196 (2015).
41. Kaur, S., Guleria, P. & Yadav, S. K. Evaluation of fermentative xylitol production potential of adapted strains of *Meyerozyma caribbica* and *Candida tropicalis* from rice straw hemicellulosic hydrolysate. *Fermentation* **9**, 181 (2023).
42. Kumar, V., Sandhu, P. P., Ahluwalia, V., Mishra, B. B. & Yadav, S. K. Improved upstream processing for detoxification and recovery of xylitol produced from corncob. *Bioresour. Technol.* **291**, 121931 (2019).
43. Ahuja, V. et al. Process development for detoxification of corncob hydrolysate using activated charcoal for xylitol production. *J. Environ. Chem. Eng.* **10**, 107097 (2022).
44. de Andrade, B. I., Jofre, F. M., Lacerda, T. M. & de Almeida Felipe, M. D. Xylitol production by *Candida tropicalis* from sugarcane bagasse and straw: An adaptive approach to improve fermentative performance. *BioEnergy Res.* **17**, 1041–1054 (2024).

Acknowledgements

This work was partially supported by the Fundamental Fund 2023 and 2024 from Thailand Science Research and Innovation (TSRI) to Chiang Mai University [Grant numbers FRB660046/0162 and MHESI6309. FB2.1/707/2566]; the Center of Excellence in Agro-Bio-Circular-Green Industry (Agro-BCG), Faculty of Agro-Industry, Chiang Mai University [CoE/RG66/67-P001]; and the CMU Proactive Researcher (Master Degree) Project, Chiang Mai University [C9CD71-155-387]. The present study was partially supported by the Thailand Research Fund (TRF) Research Team Promotion Grant, RTA, Senior Research Scholar (N42A671052). Juan Feng thanks PhD's Degree Program in Food Science and Technology, Faculty of Agro-Industry, Chiang Mai University, under the CMU Presidential Scholarship.

Author contributions

Conceptualization, J.F. and N.L.; methodology, J.F., K.P., C.M., S.S., R.N.; data curation, J.F., J.K., N.L.; investigation, J.F.; validation, J.F., Y.P., N.L.; visualization, J.F., P.R.; formal analysis, J.F., C.T., S.P., S.T., S.L.H., A.K., N.L.; writing—original draft preparation, J.F.; writing—review and editing, J.F., C.T., Y.P., P.R., S.P., J.K., S.T., K.P., C.M., S.S., R.N., A.K., N.L.; project administration, N.L.; funding acquisition, P.R., S.S., N.L.; supervision, Y.P., S.P., J.K., N.L. All authors have read and agreed to the published version of the manuscript.

Competing interests

The authors declare no competing interests.

Additional information

Correspondence and requests for materials should be addressed to N.L.

Reprints and permissions information is available at www.nature.com/reprints.

Publisher's note Springer Nature remains neutral with regard to jurisdictional claims in published maps and institutional affiliations.

Open Access This article is licensed under a Creative Commons Attribution-NonCommercial-NoDerivatives 4.0 International License, which permits any non-commercial use, sharing, distribution and reproduction in any medium or format, as long as you give appropriate credit to the original author(s) and the source, provide a link to the Creative Commons licence, and indicate if you modified the licensed material. You do not have permission under this licence to share adapted material derived from this article or parts of it. The images or other third party material in this article are included in the article's Creative Commons licence, unless indicated otherwise in a credit line to the material. If material is not included in the article's Creative Commons licence and your intended use is not permitted by statutory regulation or exceeds the permitted use, you will need to obtain permission directly from the copyright holder. To view a copy of this licence, visit <http://creativecommons.org/licenses/by-nc-nd/4.0/>.

© The Author(s) 2024